
1. Introduction

Although at one time drones were used only by the military sector, they are now used in several civilian applications areas such as smart farming[1], disaster management[2], and surveillance[3]. Earlier drones were manually and remotely operated by humans, but now flights can be pre-programmed and the drone's mission executed automatically. In this last mode, the path of the drone should be determined before the mission: the task of prior path determination is known as Coverage Path Planning[4].

Coverage Path Planning can be defined as follows: Given an area of interest, determine an optimal path of the drone allowing it to complete its mission of covering the area of interest. The objective is usually to reduce the completion time of the mission. The area of interest can be decomposed or not, depending on its regularity or its complexity. In most cases, it is decomposed into cells based on the Ground Sampling Distance (GSD), which is defined as the distance between pixel centers measured on the ground [5].

An important issue when planning the path of a drone is the energy limitation due to the small capacity of the battery. Huge amount of works tackling CPP proposed energy-aware algorithms based on some observations, mainly the fact that a drone spends a lot of time and energy making turns. Therefore, those algorithms modify conventional trajectories such as Back-and-Forth [6] and HILBERT[7]. However, the limited capacity of drones prevents them to perform large space missions. An interesting survey on coverage path planning with drone can be found in [8].

To assist drones for large-area missions, charging stations have recently been introduced [9]. When a drone runs out of energy, it lands on a charging station to recharge its battery. Scenarios in [10] use pre-defined charging station locations with only one drone. The aim is to minimize the mission completion time by deciding when the drone should stop for charging depending on the state of charge (SoC). Authors in [11] rather consider a fleet of drones and tackle the problem of coverage and energy replenishment scheduling with only one charging station at the center of the scenario. This limits the area to a radius of half the traveling distance of a drone (round trip).

To automatically surveil larger areas will require a greater number of drones. How to minimize their number and determine their optimal locations? In fact, a greater number of charging stations drastically increase the cost of the architecture for automatic surveillance. For instance, the charging pad from Heisha costs around USD 1000 while a Mavic Air drone that can be charged using this pad costs around USD 600 [12]. It is

therefore important to minimize the number of charging station in order to reduce the cost of the architecture, especially in presence of limited budget as it is the case for low-income users.

This work introduces the Single Drone and Multiple Charging Station (SD-MCS) problem. Unlike previous work focusing on the minimization of the completion time of the mission, this work rather tackles drone path planning with a priority on the economical point of view. In this formulation, an area of interest to cover is given as well as a set of potential locations for charging stations where the drone can land to recharge its battery. The aim is first to minimize the number of effectively used charging stations and then the completion time of the surveillance mission. To reach this goal, three approaches have been defined: the well-known Back and Forth (BF), Simulated Annealing (SA), and the combination of the two previous approaches namely Back and Forth Simulated Annealing (BFSA). The latter is based on the assumption that the quality of the initial solution of SA can influence the final solution. Thus, SA is combined with BF. BF generates the initial solution that is later improved by SA. To test the proposed approach, a set of 30 random topologies has been generated.

The rest of the paper is organized as follows: Section 2 presents the system model and the formulation of the Single Drone and Multiple Charging Station problem. Section 3 presents the different optimization approaches defined to solve the problem. Section 4 presents the simulation setup and compares the results. This paper ends with a conclusion and future work.

2. System Model

2.1. Scenario modelling

The area to cover is considered as a rectangular area of size D m². It is decomposed into cells as shown in Figure 1. Each cell has a unique integer identifier. The set of the cells of area is represented by A and contains $n \times m$ elements. Some cells are candidate locations for charging station deployment where drone can stop to recharge its battery. Their set is represented by C , with $C \subseteq A$. There is only one drone with a maximal capacity energy E_M . When the drone stops at charging station, it recharges its battery to E_M before leaving. The drone starts its mission at the take-off point S_t and ends it at the landing point.

The following assumptions have been made: the drone starts with the maximum energy, but this energy cannot allow it to cover the whole area; the area to be covered has

no obstacles; the wind speed is constant over the whole area; the drone flies at a constant height; and finally the ambient temperature, the taking off energy and landing energy are neglected.

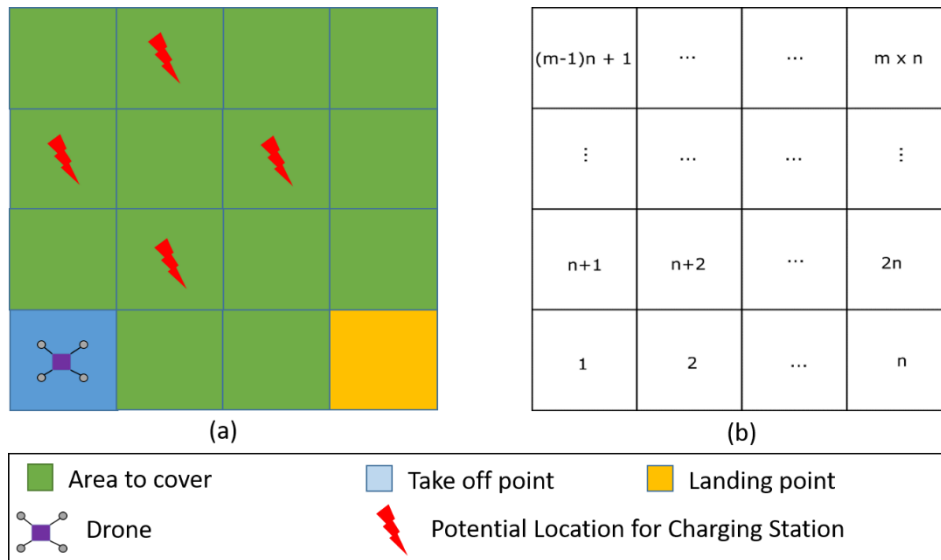


Figure 1: Problem description (a) and area decomposition (b)

2.2. Energy model

The power consumed during horizontal flight and cover has been considered approximately equivalent [13]. But it is not the case in the reality. For a better approximation, we use the energy model proposed by [10]. This model is based on empirical experiments with an estimation error around 0.4%. The power and energy are estimated respectively by (1) and (2).

$$\hat{P} = \begin{bmatrix} \beta_1 \\ \beta_2 \\ \beta_3 \end{bmatrix}^T \begin{bmatrix} \|\vec{v}_{xy}\| \\ \|\vec{a}_{xy}\| \\ \|\vec{v}_{xy}\| \|\vec{a}_{xy}\| \end{bmatrix} + \begin{bmatrix} \beta_4 \\ \beta_5 \\ \beta_6 \end{bmatrix}^T \begin{bmatrix} \|\vec{v}_z\| \\ \|\vec{a}_z\| \\ \|\vec{v}_z\| \|\vec{a}_z\| \end{bmatrix} + \begin{bmatrix} \beta_7 \\ \beta_8 \\ \beta_9 \end{bmatrix}^T \begin{bmatrix} m \\ \vec{v}_{xy} \cdot \vec{w}_{xy} \\ 1 \end{bmatrix} \quad (1)$$

$$E = \hat{P} D \quad (2)$$

Where:

- \vec{v}_{xy} and \vec{a}_{xy} indicate the speed and acceleration vectors describing the horizontal movement of the drone in m/s;
- \vec{v}_z and \vec{a}_z the speed and acceleration vectors describing the vertical movement of the drone in m/s²;
- m the weight of payload in Kg;
- \vec{w}_{xy} the vector of wind movement in the horizontal surface;
- β_1, \dots, β_9 are coefficients determined empirically;
- D is the duration.

2.3. Single Drone and Multiple Charging Station problem formulation

Formally, the SD-MCS is defined as follows: given an area to cover decomposed into a set of cells A and a set of potential locations for charging station C , determine a route R that will minimize the number of effectively used charging stations and the energy consumption of the mission. A route R is nothing else than a permutation of the elements of A . More specifically, $R = (R_1, R_2, \dots, R_{n \times m})$ with $R_i \in A, 1 \leq i \leq n \times m$.

The objective functions are given by (3) and (5). They respectively minimize the number of charging station and the energy consumption.

$$\text{Min } f_1(R) = \sum_{i=1}^n h(R_i) \quad (3)$$

$$\text{Min } f_2(R) = \sum_{i=1}^n P(R_i, R_{i+1}) t_{R_i, R_{i+1}} \quad (4)$$

Where:

$$h(R_i) = \begin{cases} 1, & R_i \in C \\ 0, & \text{otherwise} \end{cases} \quad (5)$$

- $n = \text{Card}(R)$;
- $R_i \in R$;
- $P(R_i, R_{i+1})$ is the power consumed by the drone between R_i and R_{i+1} given by eq. (1);
- $t_{R_i, R_{i+1}}$ is the time took by the drone to go from point R_i to point R_{i+1} .

3. Optimization approaches

3.1. Back and Forth

Back and Forth is the basic technique used especially in regular surfaces. It is inspired by what is called in the literature "the way of the ox", the approach is the following: when an ox trailed a plow and must cover an area, it travels along the field in a straight line, turns around, then makes a new rectilinear path adjacent to the previous one. The approach is given by Algorithm 1.

Algorithm 1: Back and Forth (BF)

Input: f_1, f_2 : Objective functions to minimize

Output: R : A route

```

1  Begin
2  | k:=0, R:=[ ]
3  | for j from 0 to n:
4  |   | for i from 0 to m:
5  |   |   | if j mod 2 = 0:
6  |   |   |   | p :=i × n + j + 1
7  |   |   |   | else:
8  |   |   |   |   | p := (m-i-1) × n + j + 1
9  |   |   |   |   | R[k] :=p
10 |   |   |   |   | k :=k + 1
11 |   |   |   | return R
12 End

```

3.2. Simulated Annealing

The SA algorithm is inspired from the annealing process in metallurgy. It proceeds as follows: an initial solution is generated, then several iterations are performed to improve this solution. A neighbour solution is generated from the previous one at each iteration. The new solution is accepted if it improves the value of the objective function. If it is not the case, the new solution is accepted with a probability depending on the current temperature T and the difference between the value of its objective function and the one of the previous solution ΔE . The probability in the SA algorithm generally follows the Boltzmann distribution given by $e^{-\frac{\Delta E}{T}}$. Since the temperature updates each time the equilibrium state is reached, the probability of accepting non-improving solutions decreases. The algorithm stops when a minimal temperature is reached. A particularised version of SA is given in Algorithm 2.

Algorithm 2: Simulated Annealing (SA)**Input:** f_1 : first objective function (number of charging station) f_2 : second objective function (energy consumption)**Output:** R : the best route found

```

1  Begin
2  |  $T := T_{initial}$ 
3  |  $R := \text{initialSolution}()$ 
4  |  $v_1 := f_1(R); v_2 := f_2(R)$ 
5  | while (stopping condition not met) do
6  |   | while (equilibrium condition not met) do
7  |   |   |  $R' := \text{newSolution}()$ 
8  |   |   |  $v_1' := f_1(R'); v_2' := f_2(R')$ ;
9  |   |   |  $\Delta E_1 := v_1' - v_1$ 
10 |   |   |  $\Delta E_2 := v_2' - v_2$ 
11 |   |   | if  $\Delta E_1 < 0$  or ( $\Delta E_1 = 0$  and  $\Delta E_2 < 0$ ) then  $R := R'$ 
12 |   |   | else accept  $R'$  if  $\Delta E_1 = 0$  with probability  $e^{-\frac{\Delta E_2}{T}}$ 
13 |   |   | Update( $T$ )
14 |   | return  $R$ 
15 End

```

InitialSolution (line 3): The initial route is obtained by generating a permutation of the cells, starting by the defined take-off point and ending by the defined landing point. Each cell has between 3 to 8 Moore neighbours. Each time a cell is included in the route, the next cell is chosen in the Moore neighbourhood of the previous cell. If it is not possible, then a random cell is generated.

Fitness functions (lines 4): the two objective functions namely f_1 and f_2 are evaluated using respectively eq. (3) and (4).

NewSolution (line 7): It is obtained from the current solution using a k-opt operator. A k-opt operator permutes k edges. A 4-opt operator is used with greater temperatures while a 2-opt is used when the temperature is close to the threshold. An illustration of the 2-opt operator application on a given route is given in Figure 2.

Stopping condition (line 5): If the current temperature is lower than a certain threshold, or the we suppose therefore having reached the optimal.

Equilibrium stage (line 6): If there is no improvement of the best solution found so far after a certain number of iteration, we suppose having reached an equilibrium state and we update the temperature.

Accepting a solution (line 11 and 12): A solution is accepted if it provides a smaller number of charging station, or if the number of charging station is the equal to the one of the best solution found so far, but with a smaller energy consumption. However, a non-improving solution with regard to energy consumption can be accepted in order to escape from local optima, but with a certain probability.

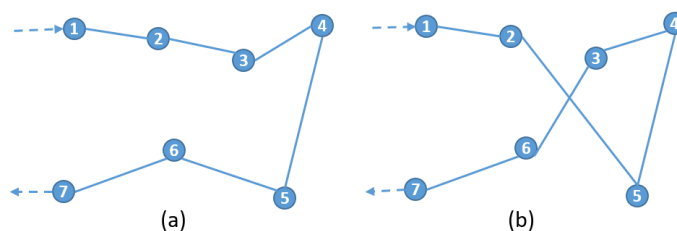


Figure 2: Application of 2-opt operator. (a) initial route: (b) neighbor route by permuting edges (2,3) and (5,6).

3.3. Back and Forth Simulated Annealing (BFSA)

BFSA is a combination of BF and SA. It is based on the idea that the initial solution of SA can improve its result. So, the initial solution is generated by BF and it is improved using SA.

4. Performance evaluation

4.1. Parameters setting

We use the parameters of the drone 3DR Solo. It has a maximum energy of $76.96Wh$. We considered that the drone flies at a speed of $0.5m/s$ and at an altitude of about $120m$. β parameters used the power in eq. (1) for 3DR solo drone are the following [10]: $\beta_1 = -1.526, \beta_2 = 3.934, \beta_3 = 0.968, \beta_4 = 18.125, \beta_5 = 96.613, \beta_6 = -1.085, \beta_7 = 0.220, \beta_8 = 1.332, \beta_9 = 433.9$. The wind speed is set to $3.88m/s$.

We generated a set of 30 random topologies of size 4×4 cells (i.e $n = m = 4$), with 4 potential charging locations. We performed 30 executions of each approach on each of these instances. Approaches have been compared with regards to three metrics namely: the feasibility, the number of charging station, and the energy consumption. A solution is a feasible if the maximum energy of the drone allows it to fly from the starting point or an intermediary charging station to the closest charging station on the route, or from the last charging station to the final landing point. All the algorithms have been implemented in Python.

4.2. Simulation results and discussion

Table 1 summarizes the results of the simulation. The data are the mean values of all the 30 runs for each instance. The best results are in bold. From the results, BFSA provides the best feasibility with a total average of 99.55% compared to 87.22% for SA and only 33.33% for BF. More specifically, BFSA provides a 100% feasibility on 27 out of 30 instances. The distribution of potential location for charging stations does not allow BF solution to be feasible on 20 out of 30 instances.

Regarding the number of charging station, BFSA again provides the best result with a total average of 3.02 charging stations, compared to 3.1 for BF and 3.14 for SA. Explicitly, BFSA provides the minimum number of charging station for all instances except instance 2 where BFSA provides 3.43 compared to 3.37 for SA. But when observing the feasibility metric for that instance, we realize that SA provides 66.67% compared to 93.33% for BFSA. That means, SA provides only 10 feasible solutions out of 30 runs when BFSA provides 28. This shows that BFSA find a feasible solution even at the expense of the number of charging station, where SA ends without finding a feasible solution. The average in terms of number of charging station of BFSA can therefore be greater than the one SA for instance 2.

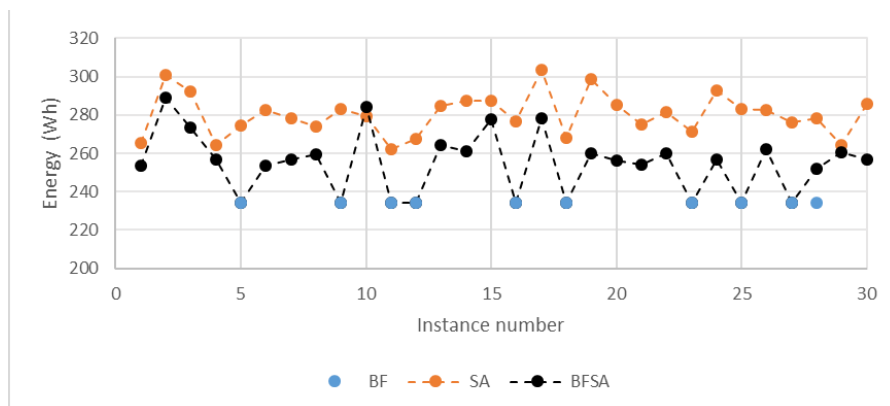


Figure 3: Mean Energy consumption

The last metric is the energy consumption. Whenever BF finds a feasible solution, the energy consumption is the smallest. But as discussed earlier, BF found only 10 feasible solutions out of 30 instances. Whenever BF finds a feasible solution, BFSA provides the same energy consumption except for instance 28 where BFSA provides 251,92Wh

compared to 234,05Wh for BF. But a look to the number of charging station shows that BFSA requires only 3 charging stations compared to 4 for BF. Since the priority is to reduce the number of charging station, BFSA' solution is considered as the best. In fact, if we considered the maximum energy of a 3DR Solo drone that is 76.96Wh, we will need at least 4 recharges to provides the required 234,05Wh. Since the drone starts with a full charge, only 3 intermediary charging stations are necessary.

To better observe the energy consumption of the different approaches, we plotted their mean values in Figure 3. From Figure 3, BFSA provides a smaller energy consumption compared to SA.

With regards on all the three metrics the difference between BFSA and SA demonstrate the impact of the initial solution on SA.

Table 1: Simulation results summarization (mean values)

	Feasibility			Number of Charging Station			Energy		
	BF	SA	BFSA	BF	SA	BFSA	BF	SA	BFSA
Inst1	0	96,67	100	_	3,03	3	_	265,48	253,40
Inst2	0	66,67	93,33	_	3,37	3,43	_	300,76	288,87
Inst3	0	80	96,67	_	3,27	3,07	_	292,15	273,55
Inst4	0	100	100	_	3	3	_	264,37	256,76
Inst5	100	96,67	100	3	3,07	3	234,05	274,56	234,05
Inst6	0	80	100	_	3,20	3	_	282,34	253,51
Inst7	0	100	100	_	3	3	_	278,41	256,88
Inst8	0	86,67	100	_	3,13	3,03	_	273,89	259,54
Inst9	100	86,67	100	3	3,17	3	234,05	283,19	234,05
Inst10	0	93,33	100	_	3,13	3,03	_	279,21	284,08
Inst11	100	93,33	100	3	3,07	3	234,05	261,92	234,05
Inst12	100	93,33	100	3	3,07	3	234,05	267,67	234,05
Inst13	0	93,33	100	_	3,07	3	_	284,84	264,13
Inst14	0	83,33	100	_	3,20	3	_	287,25	261,10
Inst15	0	86,67	96,67	_	3,13	3,03	_	287,38	277,86
Inst16	100	90	100	3	3,10	3	234,05	276,76	234,05
Inst17	0	63,33	100	_	3,40	3,03	_	303,81	278,47
Inst18	100	100	100	3	3	3	234,05	267,99	234,05
Inst19	0	63,33	100	_	3,37	3	_	298,77	260,16
Inst20	0	80	100	_	3,20	3	_	285,00	256,18

Inst21	0	100	100	_	3	3	_	275,00	253,92
Inst22	0	90	100	_	3,10	3	_	281,34	259,92
Inst23	100	93,33	100	3	3,07	3	234,05	271,52	234,05
Inst24	0	73,33	100	_	3,27	3	_	292,62	256,79
Inst25	100	83,33	100	3	3,17	3,03	234,05	283,19	234,05
Inst26	0	93,33	100	_	3,10	3	_	282,67	262,11
Inst27	100	83,33	100	3	3,20	3,03	234,05	276,29	234,05
Inst28	100	93,33	100	4	3,13	3	234,05	278,45	251,92
Inst29	0	96,67	100	_	3,03	3	_	264,37	260,40
Inst30	0	76,67	100	_	3,23	3	_	285,82	257,02
Total Average	33,33	87,22	99,55	3,1	3,14	3,02	234,05	280,23	254,43

6. Conclusion and future work

This paper has introduced the Single Drone with Multiple Charging Stations problem in which the objectives are the minimization of the number of charging station and the energy consumption of the drone. Three approaches have been proposed namely BF, SA and BFSa. Simulation results have shown the superiority of BFSa over the two others. In fact, BFSa almost always finds a feasible solution even when the others could not. In addition, BFSa provides the least expensive architecture due to the minimum number of charging station close to the optimal solution. Finally, BFSa provides in general the best energy-efficient solution.

Further investigation will be conducted to consider more realistic parameters such as wind speed and direction changing, obstacles and No-Fly Zone (NFZ). Moreover, a web interface will be designed to allow user to interact with the system directly on maps and to generate waypoints that can be imported into the drone.

7. Bibliography

- [1] P. Lottes, R. Khanna, J. Pfeifer, R. Siegwart, and C. Stachniss, "UAV-based crop and weed classification for smart farming," in *2017 IEEE International Conference on Robotics and Automation (ICRA)*, 2017, pp. 3024–3031.
- [2] B. Li, S. Patankar, B. Moridian, and N. Mahmoudian, "Planning Large-Scale Search and Rescue using Team of UAVs and Charging Stations*," in *2018 IEEE International*

Symposium on Safety, Security, and Rescue Robotics (SSRR), Philadelphia, PA, 2018, pp. 1–8, doi: 10.1109/SSRR.2018.8468631.

[3] S. Seyedi, Y. Yazicioglu, and D. Aksaray, “Persistent Surveillance With Energy-Constrained UAVs and Mobile Charging Stations,” *ArXiv Prepr. ArXiv190805727*, 2019.

[4] H. Choset, “Coverage for robotics—A survey of recent results,” *Ann. Math. Artif. Intell.*, vol. 31, no. 1–4, pp. 113–126, 2001.

[5] K. Kakaes, F. Greenword, M. Lippincott, S. Dosemagen, P. Meier, and S. A. Wich, “Drones and Aerial Observation: New Technologies for Property Rights,” *Hum. Rights Glob. Dev. Primer New Am. 2015*, pp. 514–519, 2015.

[6] Y.-S. Jiao, X.-M. Wang, H. Chen, and Y. Li, “Research on the coverage path planning of uavs for polygon areas,” in *2010 5th IEEE Conference on Industrial Electronics and Applications*, 2010, pp. 1467–1472.

[7] S. A. Sadat, J. Wawerla, and R. Vaughan, “Fractal trajectories for online non-uniform aerial coverage,” in *2015 IEEE International Conference on Robotics and Automation (ICRA)*, 2015, pp. 2971–2976.

[8] T. M. Cabreira, L. B. Brisolará, and P. R. Ferreira Jr., “Survey on Coverage Path Planning with Unmanned Aerial Vehicles,” *Drones*, vol. 3, no. 1, p. 4, Mar. 2019, doi: 10.3390/drones3010004.

[9] A. B. Junaid, Y. Lee, and Y. Kim, “Design and implementation of autonomous wireless charging station for rotary-wing UAVs,” *Aerosp. Sci. Technol.*, vol. 54, pp. 253–266, 2016.

[10] C.-M. Tseng, C.-K. Chau, K. M. Elbassioni, and M. Khonji, “Flight tour planning with recharging optimization for battery-operated autonomous drones,” *CoRR Abs170310049*, 2017.

[11] A. Trotta, M. D. Felice, F. Montori, K. R. Chowdhury, and L. Bononi, “Joint Coverage, Connectivity, and Charging Strategies for Distributed UAV Networks,” *IEEE Trans. Robot.*, vol. 34, no. 4, pp. 883–900, Aug. 2018, doi: 10.1109/TRO.2018.2839087.

[12] D. Editor, “Pilot-free, Heisha C200 drone charging solutions for automated drone applications | Droneblog.” [Online]. Available: <https://www.droneblog.com/2019/06/28/pilot-free-heisha-c200-drone-charging-solutions-for-automated-drone-applications/>. [Accessed: 25-Sep-2019].

[13] K. Dorling, J. Heinrichs, G. G. Messier, and S. Magierowski, “Vehicle routing problems for drone delivery,” *IEEE Trans. Syst. Man Cybern. Syst.*, vol. 47, no. 1, pp. 70–85, 2016.